PHYSICAL REVIEW A VOLUME 38, NUMBER 2 JULY 15, 1988

Two-electron–one-photon transition in aluminum following double-K-shell ionization

J. Auerhammer, H. Genz, A. Kumar,* and A. Richter
Institut für Kernphysik, Technische Hochschule Darmstadt, D-6100 Darmstadt, West Germany
(Received 8 February 1988)

The decay possibilities of atoms with two K-shell vacancies have been studied by bombarding a thin (465 $\mu g/cm^2$) Al target with electrons of $E_0 = 20$ keV. In addition to the more common probability involving a sequential decay [which leads to a $K^{-2} \rightarrow K^{-1}L^{-1}$ transition with the emission of a $K\alpha$ hypersatellite x ray, called the one-electron–one-photon transition (OEOP)], we have also investigated the weakly correlated two-electron–one-photon transition (TEOP) by spectroscopy of the emitted x rays using a high-resolution crystal spectrometer. The two transitions were recorded with different crystals always relative to the intensity of the $K\alpha$ line, which originates from a single-K-shell vacancy. The branching ratio $R_B = I_{TEOP}/I_{OEOP}$ was found to be $R_B = (2.2 \pm 0.8) \times 10^{-3}$, which is in good agreement with theoretical predictions, that include the electron correlation approximately and is close to previous heavy-ion induced investigations.

I. INTRODUCTION

The experimental detection of two-electron–one-photon transitions ($2e^- \rightarrow 1\gamma$) was first reported in heavy-ion collision experiments by Wölfli *et al.*[1] Since then these transitions have been detected in a variety of experiments in which the double inner-shell vacancies were produced by heavy-ion collisions,[2–6] electron-capture decay,[7] as well as proton-[8] and electron-induced[9] excitations. These experimental observations generated a great deal of interest since multielectron transitions cannot readily be described in a strict independent-particle model and it is thus expected that multiple electron transitions give valuable information on the electron-electron correlation. In fact, the study of multielectron transitions demonstrates the contribution of the configuration mixing and the interelectronic-electrostatic interactions, which couple the motions of the electrons, and it exhibits that the independent-particle model does not describe satisfactorily the complex atom. Several models were proposed to explain the decay mechanism.[10–17] They are primarily based on the configuration mixing of the electronic states of electrons and the change in the average potential of electrons in the independent-particle model and rely on various interelectron interaction perturbations. The result on the $2e^- \rightarrow 1\gamma$ transition rate varied in these calculations depending on the form of the interaction matrix used. The most recent model was proposed by Scott and Woollett[17] using the velocity as well as length forms of the interaction matrix elements. With appropriate valid approximations, both forms of the interaction matrix give similar results. The transition rates of two-electron–one-photon transitions are about four times less than the previous results of Åberg *et al.*[13]

It is the branching ratio $R_B = I_{TEOP}/I_{OEOP}$ of two-electron–one photon transitions (TEOP) that is experimentally accessible and which can directly be compared to theoretical predictions regardless of the mechanisms by which the two K-shell vacancies are created. It requires the detection of the $2e^- \rightarrow 1\gamma$ transition rate $I(K\alpha\alpha)$ and the $K\alpha$ hypersatellite transition rate $I(K\alpha_2^h)$ and its measurement thus reflects the correlation strength between inner-shell electrons. Only a few data are known, however, about the excitation and decay of double-K-vacancy states. The reason for this arises from the difficulty to identify the very weak transitions of a double-K-vacancy state. In addition, for an unambiguous determination of these transition rates a crystal spectrometer is necessary for the photon detection in order to separate the many possible satellite lines—especially in heavy-ion investigations—from the hypersatellite and $2e^- \rightarrow 1\gamma$ transitions. Despite these shortcomings, it is manifested that the few available experimental data agree with the different theoretical approaches, at least qualitatively.[2–7,10–14,16,17]

The most recent experiments on two-electron–one-photon transitions, however, were performed by Salem *et al.*[9,18] for several first transition series elements. While the double-K-shell vacancies were produced by electron bombardment, the emitted photons could be detected using a crystal spectrometer. The branching ratios deduced from these investigations were reported to be some 3 orders of magnitude higher than almost all previous experiments and theoretical calculations.

In view of this variance between electron-induced and heavy-particle-induced investigations of double-K-shell vacancy decay, the present experiment was performed to clarify the situation. Since the branching ratio decreases with increasing atomic number,[13,16,17] aluminum ($Z = 13$) was chosen as a low-Z target. It also helped us in constituting a stable thin target in view of the long hours of exposure needed.

In Sec. II we will describe shortly some of the experimental details, while more space is devoted to a detailed description of the data evaluation which turned out to be crucial for the deduction of the weak signals from the noise (Sec. III). The results obtained are discussed in Sec. IV.

II. EXPERIMENTAL PROCEDURE

The experiment was performed at our superconducting pilot accelerator facility.[19] The details of the experimental setup are described elsewhere.[19–22] Essentially, an electron gun was used as a source of an electron beam which was focused on a thin (465 $\mu g/cm^2$) Al target placed 2 m from the electron gun. After traversing through the thin target, the electrons were collected in a Faraday cup. The electron beam energy amounted to $E_0=20$ keV, which is high enough to assure only sizable contributions of additional multiple L vacancies[23] with its disturbing satellite lines, and on the other side not so high such that the weak lines searched for are concealed by the background.

The emitted characteristic radiation was studied perpendicular to the beam axis using a high-resolution flat crystal spectrometer with either a thallium acid phthalate crystal (TlAP; $2d=25.745$ Å) or a pentaerythritol crystal (PET; $2d=8.726$ Å). The energy of the transition under investigation dictated the crystal selection. While the study of the $2e^-\rightarrow 1\gamma$ transitions required the PET crystal, the $K\alpha_2^h$ transitions were recorded with the TlAP diffraction crystal. A flow proportional counter operating at a pressure of 10^5 Pa and using a mixture of argon (90%) and methane (10%) detected the x-ray photons.

To reduce the effect of current fluctuations which might generate high background intensity fluctuations, the x-ray intensity was measured per unit charge (e.g., 50 μC per step) by integrating the incident electron flux using a Faraday cup. This was crucial for the present measurements as we are dealing with exceedingly weak transitions, $I(K\alpha_2^h)/I(K\alpha)\simeq 10^{-4}$ and $I(K\alpha\alpha)/I(K\alpha)\simeq 10^{-7}$. The intensities were measured by stepping the counter along Bragg's angle in increments of $\Delta\theta=2\times 10^{-2}$ deg.

For the reduction of statistical fluctuations, the number of sweeps were increased while measuring the low-intensity lines; for example, only four sweeps were needed to obtain 2% accuracy in the determination of the intensity of the $K\alpha$ line. To obtain 5% accuracy in the intensity of $K\alpha_2^h$, 226 sweeps were needed and 1817 sweeps to reduce the statistical fluctuations and to achieve an accuracy to about 22–40 % in the intensity measurements of $2e^-\rightarrow 1\gamma$ transitions.

The electron beam was periodically checked for any defocusing that might have occurred. If any significant change was detected, the data were discarded. It took about four weeks of continuous beam time to study the $K\alpha\alpha$ transition, while the study of $K\alpha_2^h$ required only six days.

The experiment was performed in two steps. First we determined the OEOP transition probability for double-K-shell vacancies relative to a single-K-shell vacancy decay by detecting the intensity of the hypersatellite relative to the $K\alpha$ line following the procedure outlined previously.[21] Accordingly, the intensity of the TEOP transition was detected again relative to the $K\alpha$ radiation.

III. ANALYSIS AND RESULTS

Figure 1 exhibits the total spectrum obtained by summing the above-mentioned 226 single spectra taken to deduce the hypersatellite intensity between 1.60 and 1.64 keV relative to the $K\alpha$ line at 1.4867 keV. A least-squares-fitting procedure was adopted to determine the peak position, intensity, and width of the $K\alpha$ transition (line A) and its satellite (line B) using a combination of a Gaussian and Breit-Wigner function. In order to untangle the spectrum it became necessary to subtract the satellites (lines C,E,F,G) which could not be resolved in the present experiment. For this purpose we assumed a Gaussian shape for each of the lines centered at energies reported by Keski-Rahkonen *et al.* (Ref. 24) for electron impact energies of $E_0=3.25$ keV. Since the intensities of these transitions decrease with electron energy,[23,25] the intensities of the satellites produced at $E_0=20$ keV as in the present work reduce to about 50% of the value at 3.25 keV. The result of the fitting procedure is shown in the middle part of Fig. 1 on the right-hand side designated by S. The hypersatellite line D and its satellites H and I were determined by applying the same fitting function and the energies of Ref. 24. The shaded area of line D represents the transition searched for. Energies[24] and the intensities of all lines are compiled in Tables I and II, where D is the hypersatellite of interest.

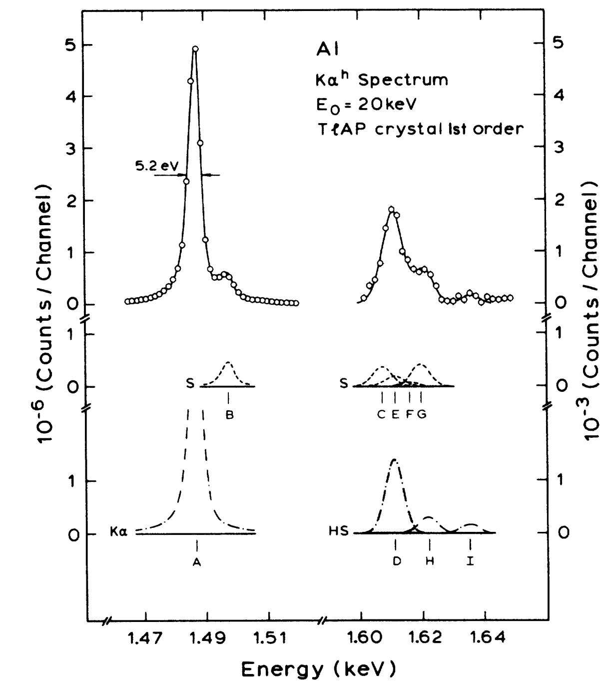

FIG. 1. The upper part shows the aluminum $K\alpha$ (left-hand side) and $K\alpha^h$ (right-hand side) background eliminated spectra obtained by bombarding a thin (465 $\mu g/cm^2$) Al target with electrons of 20 keV energy using a flat TlAP crystal. The solid line represents the result of a fitting procedure explained in text. The decomposition of the spectra was achieved by separating those contributions caused by satellites S from the hypersatellite transitions HS. The lines B, C, E, F, and G, as indicated in the middle part of the figure, denote the satellites characterized in Table I, whose intensities were taken from the work of Ref. 24 scaled down (Refs. 23 and 25) to the impact energy of the present investigation. In the lower part of the figure the $K\alpha_2^h$ transition searched for is displayed shaded D together with two satellites of the hypersatellite H,I and the $K\alpha$ transition A.

TABLE I. Energies of the designated spectral lines of aluminum given absolutely (Ref. 24) and relative to the $K\alpha_2$ line (1486.27 eV). Line D denotes the hypersatellite line of interest.

	Designated transition		Energy (eV)	ΔE (eV)
A	$K^{-1} \to L^{-1}$	$K\alpha_1$	1486.7	0.4
B	$K^{-1}L^{-1} \to L^{-2}$	$K\alpha_{3,4}$	1497.3	11.0
C	$K^{-1}L^{-2} \to L^{-2}M^{-1}$	$K\beta^{\mathrm{VII}}$	1607.4	121.1
D	$K^{-2} \to K^{-1}L^{-1}$	$K\alpha_2^h$	1611.0	124.7
E	$K^{-1}L^{-2} \to L^{-2}M^{-1}$	$K\beta^{\mathrm{VIII}'}$	1611.4	125.1
F	$K^{-1}L^{-2} \to L^{-2}M^{-1}$	$K\beta^{\mathrm{VIII}'}$	1612.1	125.8
G	$K^{-1}L^{-2} \to L^{-2}M^{-1}$	$K\beta^{\mathrm{VIII}}$	1618.3	132.0
H	$K^{-2}L^{-1} \to K^{-1}L^{-2}$	$K\alpha_2^h(L^{-1})$	1621.0	134.7
I	$K^{-2}L^{-2} \to K^{-1}L^{-3}$	$K\alpha_2^h(L^{-2})$	1636.0	149.7

The observed two-electron–one-photon transitions are shown in Fig. 2—lines J through Q—together with the $K\alpha$ line relative to which the spectra were collected. The much higher resolution of the $K\alpha$ line originates from the use of a PET crystal during these runs which enabled the detection of the weak $K\alpha\alpha$ transitions. The satellite (B) observed with the TlAP crystal (Fig. 1) lies above the data range of the $K\alpha$ line and is thus not present in Fig. 2. The separation of the spectrum was achieved by fitting Gaussians to the lines L through Q. The energies and intensities resulting from this least-squares-fitting procedure are listed in Tables III and IV. The transition of interest (line L) is displayed again shaded.

The reported intensities were corrected for absorption in the target, the crystal reflectivity and the detector efficiency (Table V). Since fluorescence yields of multiple ionized atoms are known only for a few elements[26] the ratios deduced for neon were applied for the satellites B with $\omega^{-1}/\omega^{-0}=1.10$ and C,E,F,G with $\omega^{-2}/\omega^{-0}=1.22$ and the hypersatellites D,H,I with $\omega_{\bar{H}}^{0}/\omega^{-0}=1.14$, $\omega_{\bar{H}}^{1}/\omega^{-0}=1.34$, and $\omega_{\bar{H}}^{2}/\omega^{-0}=1.41$, respectively. Since no fluorescence yields are available for two-electron–one-photon transitions, we adopted in a first approach a value which characterizes the transition from the initial K^{-2} to the final L^{-2} state via a $K^{-1}L^{-1}$ state yielding $\omega_{2e\to 1\gamma} \simeq (\omega^{-1}/\omega^{-0})(\omega_{\bar{H}}^{1}/\omega^{-0})=1.46$.

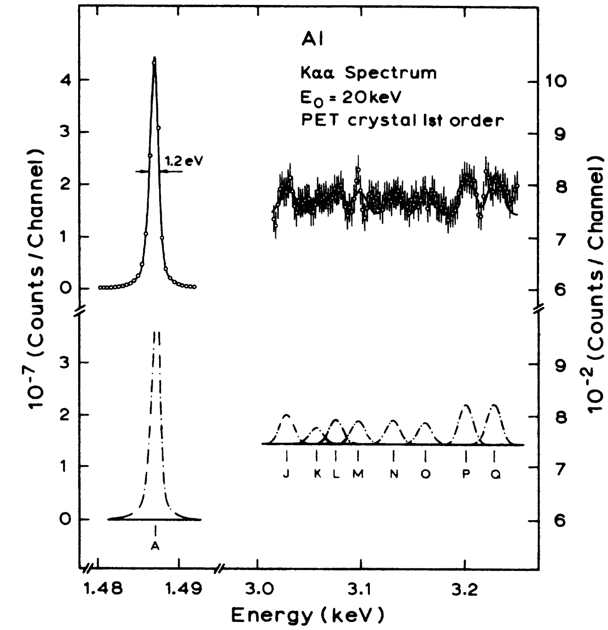

FIG. 2. Aluminum $K\alpha$ and the two-electron–one-photon spectra are displayed in the upper part of the figure for the same conditions described in Fig. 1 but with the use of a PET crystal (note the different energy scales on the left- and right-hand side). The solid line represents the result of a fitting procedure explained in the main text. The decomposition of the spectrum led to a number of transitions, where only lines J and K could not be identified while L through Q belong to $2e^- \to 1\gamma$ transitions. The designations of the lines are listed in Table III. The $2e^- \to 1\gamma$ transition for the decay of the K^{-2} state, which is searched for, is indicated by the shaded area L.

The total error of the hypersatellite intensity (line D) as quoted in Table II is caused by uncertainties in the fitting procedure (2%–5%), fluorescence yields (7%), corrections of absorption (10%), crystal reflectivity (8%), and detector efficiency (2%), and also by a systematical uncertainty originating from the subtraction of the satellite lines C,E,F,G (10%). In case of the $2e^- \to 1\gamma$ transitions

TABLE II. Intensities of the designated spectral transitions $I(X)$, $(X=B,C,\ldots,I)$ of aluminum relative to the $K\alpha_{1,2}$ line. Line D denotes the hypersatellite line of interest.

	Designated transition	$10^4 I(X)/I(K\alpha_{1,2})$ Present work $E_0=20$ keV	Ref. 24 $E_0=3.25$ keV	Ref. 24 $E_0=12$ keV
B	$K\alpha_{3,4}$	1032.00±62.0	1025.00	
C	$K\beta^{\mathrm{VII}}$	1.23±0.4	2.46	
D	$K\alpha_2^h$	5.30±0.9		1.4±0.2[a]
E	$K\beta^{\mathrm{VIII}'}$	0.60±0.2	1.20	
F	$K\beta^{\mathrm{VIII}'}$	0.21±0.07	0.42	
G	$K\beta^{\mathrm{VIII}}$	0.96±0.31	1.92	
H	$K\alpha_2^h(L^{-1})$	1.40±0.2		0.6±0.1[a]
I	$K\alpha_2^h(L^{-2})$	0.02±0.007		

[a]These values were deduced by subtracting the satellite intensities measured at 3.25 keV (for discussion see the main text).

TABLE III. Energy difference $\Delta E = E(K\alpha\alpha) - 2E(K\alpha_1)$ in eV for the designated transitions in aluminum. Line L is the one of interest.

	Designated transition	ΔE (eV) Experiment Present work	Ref. 6	Theory Ref. 15	Ref. 13
J		56.1			
K		84.8			
L	$K^{-2} \rightarrow L^{-2}$	103.4	102.0	93.0	78.0
M	$K^{-2}L^{-1} \rightarrow L^{-3}$	125.5		118.0	
N	$K^{-2}L^{-2} \rightarrow L^{-4}$	159.0		148.0	101.0
O	$K^{-2}L^{-3} \rightarrow L^{-5}$	189.9		180.0	
P	$K^{-2}L^{-4} \rightarrow L^{-6}$	229.7		216.0	
Q	$K^{-2}L^{-5} \rightarrow L^{-6}M^{-1}$	256.7		256.0	

(line L) the first mentioned error amounts even to 20–30 % and the one for the fluorescence yield to 15%, while the uncertainty in the absorption is about 2% and all other ones are of the same order of magnitude. A total error of 35% is adopted which yields an overall uncertainty of 38% for the branching ratio.

IV. RESULTS AND DISCUSSION

The results concerning the intensities of the hypersatellites and two-electron–one-photon transitions are combined in Tables II and IV. We will concentrate on the two relevant transitions D and L only.

A. Intensity of hypersatellite lines

The observed Al $K\alpha^h$ transition contains only the $K\alpha_2^h$ transition because the $K\alpha_1^h$ transition is forbidden in the strong L-S coupling scheme since the $1s^{-2}\,{}^1S_0 \rightarrow 1s^{-1}2p^{-1}\,{}^3P_1$ ($K\alpha_1^h$) spin-flip transition is not allowed. As indicated in Table II (line D), the observed intensity $I(K\alpha_2^h)/I(K\alpha)$ is nearly four times higher than the value previously reported.[24] It is worthwhile to mention, however, that the former experiment was performed at a lower electron impact energy (12 keV). The satellites that occur at nearly the same energy (compare Fig. 1, lines C, E, F, and G) were taken into account also, although their intensity was considered to be equal to the one determined at a much lower electron impact energy (3.25 keV). Since this intensity decreases, however, with electron impact energy,[23,25] its contribution was overestimated and thus the value quoted is too low by the same amount. This fact, however, does not account for the total difference to the present experiment and thus the origin of the discrepancy is not well evident.

The value of $I(K\alpha^h)/I(K\alpha)$ from a heavy-ion collision experiment[2] exceeds our result by more than a factor of 30. This result is not presented in Table II. Since the excitation of an atom depends on the nature of the projectile and its energy, it is meaningless to compare the $I(K\alpha^h)/I(K\alpha)$ ratio in various experiments using different excitation techniques. Especially in heavy-ion collisions the probability of multiple inner-shell vacancies is enhanced in comparison to electron ionization, which would at least explain in part the large reported value in Ref. 2 in comparison with the present value.

The intensity of $K\alpha^h(L^{-1})$ relative to $K\alpha^h(L^{-0})$ is about 26% from the present work while Keski-Rahkonen *et al.* (Ref. 24) report 42% for this ratio which is—considering the fairly large uncertainties—still of the same order.

B. Two-electron–one-photon transition

As has been mentioned earlier, the designation of the observed transitions is solely based on the energy criterion where the predicted energy values by Tanis *et al.*

TABLE IV. Intensities of the designated $2e^- \rightarrow 1\gamma$ spectral transitions of aluminum relative to the $K\alpha_{1,2}$ and to the $K\alpha_2^h$ line. Line L is of special interest.

	Designated transition	$10^6 I[K\alpha\alpha(L^{-n})]/I(K\alpha_{1,2})$	$10^3 I(K\alpha\alpha)/I(K\alpha_2^h)$ Experiment Present work	Ref. 2	Theory Ref. 11	Ref. 16	Ref. 12	Ref. 13
J		1.36±0.48						
K		0.72±0.25						
L	$K\alpha\alpha$	1.14±0.40	2.2±0.8	1.04±0.19	0.8	1.0	1.5	1.4
M	$K\alpha\alpha(L^{-1})$	1.07±0.37						
N	$K\alpha\alpha(L^{-2})$	1.17±0.41						
O	$K\alpha\alpha(L^{-3})$	1.09±0.38						
P	$K\alpha\alpha(L^{-4})$	2.02±0.71						
Q	$K\alpha\alpha(L^{-5})$	0.95±0.33						

TABLE V. Corrections for x-ray absorption in the target (Abs), efficiency of the proportional counter (ϵ), and reflectivity of the crystal (R) applied for the designated spectral transition rates. Lines D and L are of special interest.

	Designated transition	Abs	ϵ	$10^4 R$
A	$K\alpha_{1,2}$	0.878	0.572	1.40[a] 2.45[b]
B	$K\alpha_{3,4}$	0.881	0.575	1.40[a]
C	$K\beta^{\text{VII}}$	0.340	0.590	1.40[a]
D	$K\alpha_2^h$	0.342	0.590	1.40[a]
E	$K\beta^{\text{VIII}'}$	0.342	0.590	1.40[a]
F	$K\beta^{\text{VIII}'}$	0.342	0.590	1.40[a]
G	$K\beta^{\text{VIII}}$	0.344	0.590	1.40[a]
H	$K\alpha_2(L^{-1})$	0.345	0.600	1.40[a]
I	$K\alpha_2(L^{-2})$	0.351	0.600	1.40[a]
J		0.780	0.380	1.87[b]
K		0.784	0.373	1.87[b]
L	$K\alpha\alpha$	0.787	0.369	1.87[b]
M	$K\alpha\alpha(L^{-1})$	0.790	0.364	1.87[b]
N	$K\alpha\alpha(L^{-2})$	0.795	0.356	1.87[b]
O	$K\alpha\alpha(L^{-3})$	0.799	0.349	1.87[b]
P	$K\alpha\alpha(L^{-4})$	0.804	0.340	1.87[b]
Q	$K\alpha\alpha(L^{-5})$	0.808	0.733	1.87[b]

[a]Thallium acid phthalate crystal.
[b]Pentaerythritol crystal.

(Ref. 15) are used as the guideline for the present assignments of the transitions. While the previous experimental determination[6] falls within the limits of the uncertainties of the present measurement of $K\alpha\alpha$, the theoretical predictions are systematically about 10 keV lower (Table III). Since there is no other observation of $K\alpha\alpha$ (L^{-n};$n=1,\ldots,5$), our results cannot be compared. It is worthwhile to mention here that such transitions have not been observed for any element so far. It also shows clearly that the use of a crystal spectrometer is essential to separate the different lines which do carry even in electron-excited double-K-shell vacancy ionizations a considerable strength.

As mentioned previously, the intensity ratio $I(K\alpha\alpha)/I(K\alpha^h)$, as shown in column 3 of Table IV, depends on the mode of excitation which gives rise to various populations of the initial configuration states of the excited atom. It is thus uninformative to compare the present measurement with a heavy-ion induced experiment.[2]

The branching ratio $R_B = I_{\text{TEOP}}/I_{\text{OEOP}}$ which is obtained from the two independent measurements of $I(K\alpha_2^h)/I(K\alpha)$ and $I(K\alpha\alpha)/I(K\alpha)$ was found for Al to be

$$R_B = I(K\alpha\alpha)/I(K\alpha_2^h) = (2.2\pm0.8)\times10^{-3} \ .$$

This value differs within the error limits from our previously reported number[27] where the satellite intensities (compare Fig. 1) were not taken into account. It is also somewhat larger than the value reported by Stoller *et al.* (Ref. 2) and nearly one order of magnitude larger than the observations made by Schuch *et al.* (Ref. 5) using heavy-ion ionization. In general, however, it is possible to compare the results of R_B obtained by heavy-ion induced excitation with the present experiment, since the $K\alpha\alpha$ and $K\alpha^h$ transitions originate from the same initial-state configuration. We have listed in Table IV the R_B value obtained by Stoller *et al.* (Ref. 2) only, since only those data can be compared that have been deduced from high-resolution spectra in which the various $K\alpha\alpha$ (L^{-n}; $n=0,1,2,\ldots$) transitions can be separated (see Fig. 2).

Finally, the present result is compared with various theoretical predictions (Table IV). It becomes apparent that our value is in accordance with the calculations by Gavrila and Hansen (Ref. 12) and by Åberg *et al.* (Ref. 13) and somewhat larger than the results obtained by Vinti (Ref. 11) and Khristenko (Ref. 16). This clearly reflects the importance of the electron correlation which has approximately been taken into account in the work by Åberg *et al.* using the shakedown model to calculate the average $1s^{-2}\rightarrow 2s^{-1}2p^{-1}$ electric dipole transition rate. The approach chosen by Gavrila and Hansen (Ref. 12) yields a similar result. It circumvents the inclusion of correlation in the proper sense by applying a single particle model that takes the relaxation between the initial and final state into account. The shortcomings of the calculation by Vinti and Khristenko have been pointed out previously.[12] Finally, it is noted that the present observations do not confirm the results obtained by Scott and Wollett (Ref. 17) which yield transition rates that are four times less than the values of Åberg.

V. CONCLUSION

The intensities of aluminum hypersatellites are measured with accuracy in electron excitation method. The intensity ratio $I(K\alpha_2^h)/I(K\alpha_{1,2})$ is measured at 20 keV electron impact energy and found to be some four times higher than the previous result using a similar technique at a different impact energy (12 keV). This discrepancy can be explained only partially.

Two-electron–one-photon transitions in various L-shell configurations were detected for aluminum. The energies of $2e^- \rightarrow 1\gamma$ transitions as observed in the present work agree with the results of previous experiments and theoretical calculations.

The branching ratio R_B is also close to the previous experiments using Al and in agreement with theoretical predictions. It confirms the expected influence of the electron-electron correlation and contradicts the results of Salem *et al.* (Ref. 9) obtained for several transition elements. Due to the improved technique used in the present experiment, a value for the branching ratio is obtained which could be used to refine the theoretical models for the decay scheme of the multiionized atom.

ACKNOWLEDGMENTS

This work has been supported by Deutsche Forschungsgemeinschaft. One of us (A.K.) is thankful to the Alexander von Humboldt Foundation for partial support of the present work.

*Present address: Department of Physics and Astronomy, California State University, Long Beach, CA 90840.

[1]W. Wölfli, C. Stoller, G. Bonani, M. Suter, and M. Stöckli, Phys. Rev. Lett. **35**, 656 (1975).
[2]C. Stoller, W. Wölfli, B. Bonani, M. Stöckli, and M. Suter, Phys. Rev. A **15**, 990 (1977).
[3]T. P. Hoogkamer, P. Woerlee, F. W. Saris, and M. Gavrila, J. Phys. B **9**, L145 (1976).
[4]J. Volpp, R. Schuch, G. Nolte, and H. Schmidt-Böcking, J. Phys. B **12**, L325 (1979).
[5]R. Schuch, G. Gaukler, and H. Schmidt-Böcking, Z. Phys. A **290**, 19 (1979).
[6]A. R. Knudson, K. W. Hill, P. G. Burkhalter, and D. J. Nagel, Phys. Rev. Lett. **37**, 679 (1976).
[7]Y. Isozumi, Phys. Rev. A **22**, 1948 (1980).
[8]M. S. A. L. Al-Ghazi, J. Birchall, and J. S. C. McKee, Phys. Rev. A **25**, 3072 (1982).
[9]S. I. Salem, A. Kumar, and B. L. Scott, Phys. Rev. A **29**, 2634 (1984).
[10]V. I. Safronova and V. S. Senachenko, J. Phys. B **14**, 603 (1981).
[11]J. P. Vinti, Phys. Rev. **42**, 632 (1932).
[12]M. Gavrila and J. E. Hansen, J. Phys. B **11**, 1353 (1978).
[13]T. Åberg, K. A. Jamison, and P. Richard, Phys. Rev. Lett. **37**, 63 (1976).
[14]W. L. Luken, J. S. Greenberg, and P. Vincent, Phys. Rev. A **15**, 2305 (1977).
[15]J. A. Tanis, J. M. Feagin, W. W. Jacobs, and S. M. Shafroth, Phys. Rev. Lett. **38**, 868 (1977).
[16]S. V. Khristenko, Phys. Lett. **59A**, 202 (1976).
[17]B. L. Scott and E. L. Woollett, Phys. Rev. A **32**, 937 (1985).
[18]S. I. Salem, A. Kumar, B. L. Scott, and R. D. Ayers, Phys. Rev. Lett. **49**, 1240 (1982).
[19]T. Grundey, H. Heinrichs, U. Klein, G. Müller, G. Nissen, H. Piel, H. Genz, H.-D. Gräf, M. Janke, A. Richter, M. Schanz, E. Spamer, and O. Titze, Nucl. Instrum. Methods **224**, 5 (1984).
[20]S. Reusch, H. Genz, W. Löw, and A. Richter, Z. Phys. D **3**, 379 (1986).
[21]J. Auerhammer, H. Genz, G. Kilgus, A. Kumar, and A. Richter, Phys. Rev. A **35**, 4505 (1987).
[22]J. Auerhammer, H. Genz, and A. Richter, Z. Phys. D **7**, 301 (1988).
[23]W. Löw, H. Genz, A. Richter, and K. G. Dyall, Phys. Lett. **100A**, 130 (1984).
[24]O. Keski-Rahkonen, E. Mikkola, K. Reinikainan, and M. Lehkonen, J. Phys. C **18**, 2961 (1985).
[25]W. Löw, Ph.D. thesis, Technische Hochschule Darmstadt, 1982.
[26]O. Benka, Nucl. Instrum. Methods B **4**, 279 (1984).
[27]A. Kumar, J. Auerhammer, H. Genz, and A. Richter, J. Phys. (Paris) Colloq. **48**, C9-665 (1987).

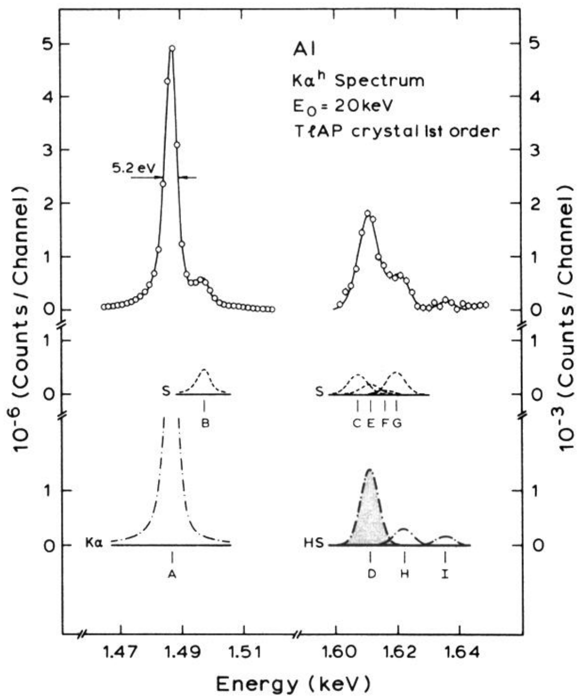

FIG. 1. The upper part shows the aluminum $K\alpha$ (left-hand side) and $K\alpha^h$ (right-hand side) background eliminated spectra obtained by bombarding a thin (465 $\mu g/cm^2$) Al target with electrons of 20 keV energy using a flat TlAP crystal. The solid line represents the result of a fitting procedure explained in text. The decomposition of the spectra was achieved by separating those contributions caused by satellites *S* from the hypersatellite transitions *HS*. The lines *B*, *C*, *E*, *F*, and *G*, as indicated in the middle part of the figure, denote the satellites characterized in Table I, whose intensities were taken from the work of Ref. 24 scaled down (Refs. 23 and 25) to the impact energy of the present investigation. In the lower part of the figure the $K\alpha_2^h$ transition searched for is displayed shaded *D* together with two satellites of the hypersatellite *H*,*I* and the $K\alpha$ transition *A*.